Journal of Archaeological Science: Reports 9 (2016) 309–319

Contents lists available at ScienceDirect

Journal of Archaeological Science: Reports

journal homepage: www.elsevier.com/locate/jasrep

A comprehensive chronology of the Neanderthal site Moula-Guercy, Ardèche, France

Malte Willmes [a,*], Rainer Grün [a,1], Katerina Douka [b], Véronique Michel [c,d], Richard A. Armstrong [a], Alexa Benson [a,2], Evelyne Crégut-Bonnoure [e,f], Emmanuel Desclaux [g], Fang Fang [a], Leslie Kinsley [a], Thibaud Saos [h], Alban R. Defleur [i]

[a] Research School of Earth Sciences, The Australian National University, 142 Mills Road, 2601 Acton, ACT, Australia
[b] Research Laboratory for Archaeology and the History of Art, University of Oxford, Dyson Perrins Building, South Parks Road, OX1 3QY Oxford, UK
[c] Université Nice Côte d'Azur, CNRS, CEPAM, SJA3, 24 Avenue des Diables bleux, 06357 Nice, Cedex 4, France
[d] Université Nice Côte d'Azur, CNRS, OCA, IRD, Géoazur, France
[e] Museum Réquien, 67 Rue Joseph Vernet, Avignon, France
[f] UMR 5608 TRACES (UTM), 5 allées Antonio Machado, 31058 Toulouse Cedex 1, Toulouse, France
[g] Laboratoire départemental de Préhistoire du Lazaret – UMR7194 CNRS, 33 Bis Boulevard Franck Pilatte, 06300 Nice, France
[h] Université de Perpignan Via Domitia, UMR-CNRS 7194, EPCC Centre Européen de Recherches Préhistoriques, Avenue Léon-Jean Grégory, 66720 Tautavel, France
[i] CNRS UMR 5276 - Laboratoire de Géologie de Lyon, Ecole Normale Supérieure de Lyon, 46, Allée d'Italie, 69364 Lyon Cedex 07, France

ARTICLE INFO

Article history:
Received 7 March 2016
Received in revised form 8 August 2016
Accepted 8 August 2016
Available online xxxx

Keywords:
Fossil teeth
Radiocarbon dating
U-series dating
ESR dating
Biostratigraphy
Neanderthal

ABSTRACT

The Baume (cave) Moula-Guercy, in southeast France, contains an important sedimentary sequence, which includes the remains of a cannibalised group of Neanderthals. The chronology of the upper layers of the cave is currently constrained by a thermoluminescence date of 72 ± 12 ka, obtained from a tephra deposit (layer VI). The middle and lower layers of the cave have been constrained by biostratigraphy, pointing towards the end of MIS 5 for the Neanderthal bearing layer XV. In order to refine the chronology of the site, we applied radiocarbon, $^{40}Ar/^{39}Ar$, U-series and ESR dating analyses. Radiocarbon dates on bone samples from layer IV showed ages older than 50 ka. $^{40}Ar/^{39}Ar$ dating on sanidines from tephra of layer VI revealed, that these volcanic minerals derived probably from the Hercynian basement, and thus provided no tangible chronological constrain. Combined CSUS/ESR results on faunal teeth place layer IV at the end of MIS 3 to MIS 4, in agreement with the radiocarbon dates and in stratigraphic order with the thermoluminescence age for layer VI. Layer VIII, with only one sample, is tentatively placed to the end of MIS 4. The age estimates for layer XIV are not conclusive, preventing an age estimation for this layer. The younger age result for layer XIV does not agree with the stratigraphy and biostratigraphy of the site and more direct dating of material from this layer is needed to resolve this discrepancy. Located just below, the crucial Neanderthal bearing layer XV is placed to the end of MIS 5 and younger than MIS 6, in agreement with the climatological and chronological deductions from the stratigraphy and biostratigraphy of the site. Direct U-series analyses on two Neanderthal teeth agree with an age for layer XV corresponding to at least MIS 5 *sensu lato*. The U-series results on the Neanderthal tooth 3525 show that U-mobilisation even into small teeth is highly complex, but nevertheless give an indication that this sample corresponds to MIS 5e. This is in agreement with the CSUS/ESR results from faunal teeth as well as the stratigraphy and biostratigraphy of the cave. The refined chronology corroborates the existing stratigraphic and biostratigraphic framework. Moula-Guercy layer XV, with its many human remains showing cannibalism, now stands as a reference site for this particular aspect of human behaviour.

1. Introduction

1.1. The site of Moula-Guercy

The Baume (cave) Moula-Guercy is located 80 m above the west bank of the Rhône River near the city of Valence, southeastern France, in the parish of Soyons, Ardèche (Fig. 1). The site was discovered in 1970 and excavated between 1975 and 1982 by P. Payen

* Corresponding author at: Department of Wildlife, Fish, & Conservation Biology, University of California Davis, CA, USA.
E-mail address: malte.willmes@googlemail.com (M. Willmes).
[1] Now at: Research Centre of Human Evolution, Environmental Futures Research Institute, Griffith University, Nathan, QLD 4111, Australia.
[2] Now at: Department of Human Evolution, Max Planck Institute of Evolutionary Anthropology, 04103 Leipzig, Germany.

http://dx.doi.org/10.1016/j.jasrep.2016.08.003
2352-409X/

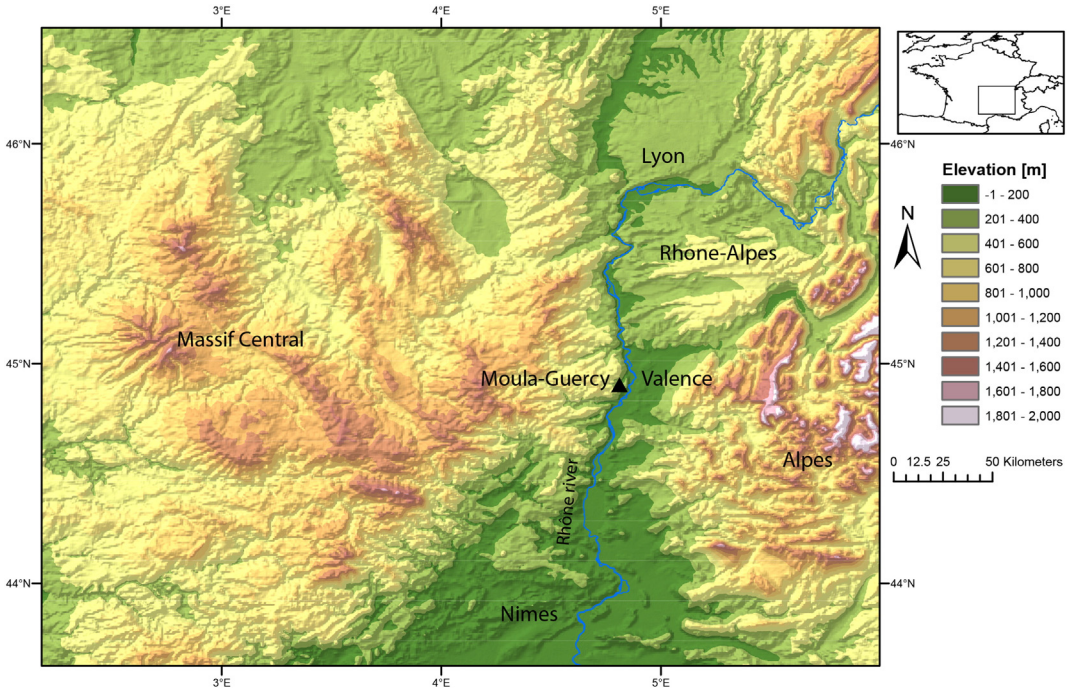

Fig. 1. Geographical location of the Moula-Guercy Cave. Elevation data from worldclim.org (Hijmans et al., 2005).

(Crégut-Bonnoure and Guérin, 1986; Defleur, 1989; Payen et al., 1990). After a 1 m^2 test pit was dug in 1991, systematic excavations were carried out between 1993 and 1999 by A.R. Defleur. The earlier excavation from 1975 to 1982 removed about 100 m^3 of Mousterian sediments, destroying much of the upper section of the sequence, and reached down to the mid of layer XIV (Fig. 2). This campaign yielded two Neanderthal teeth that cannot be attributed with certainty to any layer. The 1991 test pit, starting at the base of the previous excavation, >5 m below the surface, yielded 13 Neanderthal remains, some of which showed cut marks and evidence of fractures of fresh bones (Defleur et al., 1993). The follow-up excavations yielded 119 human remains from layer XV representing at least six individuals: two adults - a large older male individual and a smaller one, possibly a female, two adolescents most likely female and two children aged between four and seven years (Defleur, 1999).

Anatomical studies on the crania and mandibles, teeth (Hlusko et al., 2013) and postcranial remains (Mersey et al., 2013a, 2013b), identified characteristic Neanderthal traits, while no evidence for the presence of any of other hominid taxa was found. Detailed forensic examinations on the human remains showed that all individuals, including a 4-year-old child, had been cannibalised. This assessment is based on the similar processing observed for human and red deer remains at the site. The skulls had been skinned and the pericranium removed before fracturing. All muscles from the crania, mandibles, limbs were removed. Shoulders, elbows, feet and hands were disarticulated and all bones with marrow were systematically fragmented, while those without marrow were not (Defleur, 1999; Defleur et al., 2014). DNA analyses of the material did not yield any results due to the difficulty in extracting any organic material from the examined fossils (pers. comm. S. Pääbo to A.R. Defleur, 15 August 2013). Human remains were only found in Layer XV, apart from Neolithic graves dug into upper layers, and the two Neanderthal teeth uncovered during the initial excavation.

Moula-Guercy is situated on the west side of the Rhône valley, Ardèche, among numerous Palaeolithic sites associated with Neanderthal occupation. Extensive studies on the Middle Palaeolithic assemblages of the Ardèche region have shown a great diversity of Neanderthal subsistence and occupation patterns, ranging from long-term residential camps to short-term hunting and stopover camps (Daujeard and Moncel, 2010). A detailed taphonomic analysis of the larger mammals from Moula-Guercy Layer XV (Valensi et al., 2012) concluded that many animal remains were brought to the site for consumption. Based on the relatively small amount of lithic material (Defleur, 2015) and based on the animal remains found at Moula-Guercy this site is considered to have been used as specialized, short-term hunting camp (Daujeard and Moncel, 2010; Saos et al., 2014; Valensi et al., 2012).

The aim of this study is to corroborate the existing chronological framework of the whole sedimentary sequence, in particular the crucial layer XV, using a range of dating techniques. Direct dating of these layers will allow us to understand Moula-Guercy in the regional chronologic context (Daujeard and Moncel, 2010; Defleur et al., 2001; Michel et al., 2013; Richard et al., 2015) and contribute to the investigation into the changes of subsistence and occupation patters with time. The following sections first outline the already established chronology, and then provide the results of the new radiocarbon, $^{40}Ar/^{39}Ar$, U-Series, and ESR dating analyses.

1.2. Stratigraphy

The stratigraphy of Moula-Guercy has been investigated in detail by Saos et al. (2014) and an overview is shown in Fig. 2. All depths refer to below datum and the bedrock has not been reached during the excavations. The description of the excavated sections and the sedimentological analysis of the cave infilling (Saos, 2003; Saos et al., 2014) allow the distinction of three major depositional complexes, which are further subdivided into layers, some of which include archaeological layers. The lower stratigraphic complex comprises layers XX to XVI from the base to 610 cm below datum, and is only exposed in the pit near the west wall (see inset in Fig. 2). The sediments are mainly sandy with limestone blocks. The middle stratigraphic complex (from 610 cm to about 400 cm) begins with layer XV, which yielded numerous human remains, and ends with layer XI. All layers are sloped (up to 30°) towards the north. The upper stratigraphic complex (from 400 cm to 0 cm) includes layers X – III. It is only exposed at the entrance of the cave, since it was strongly affected by the early excavations.

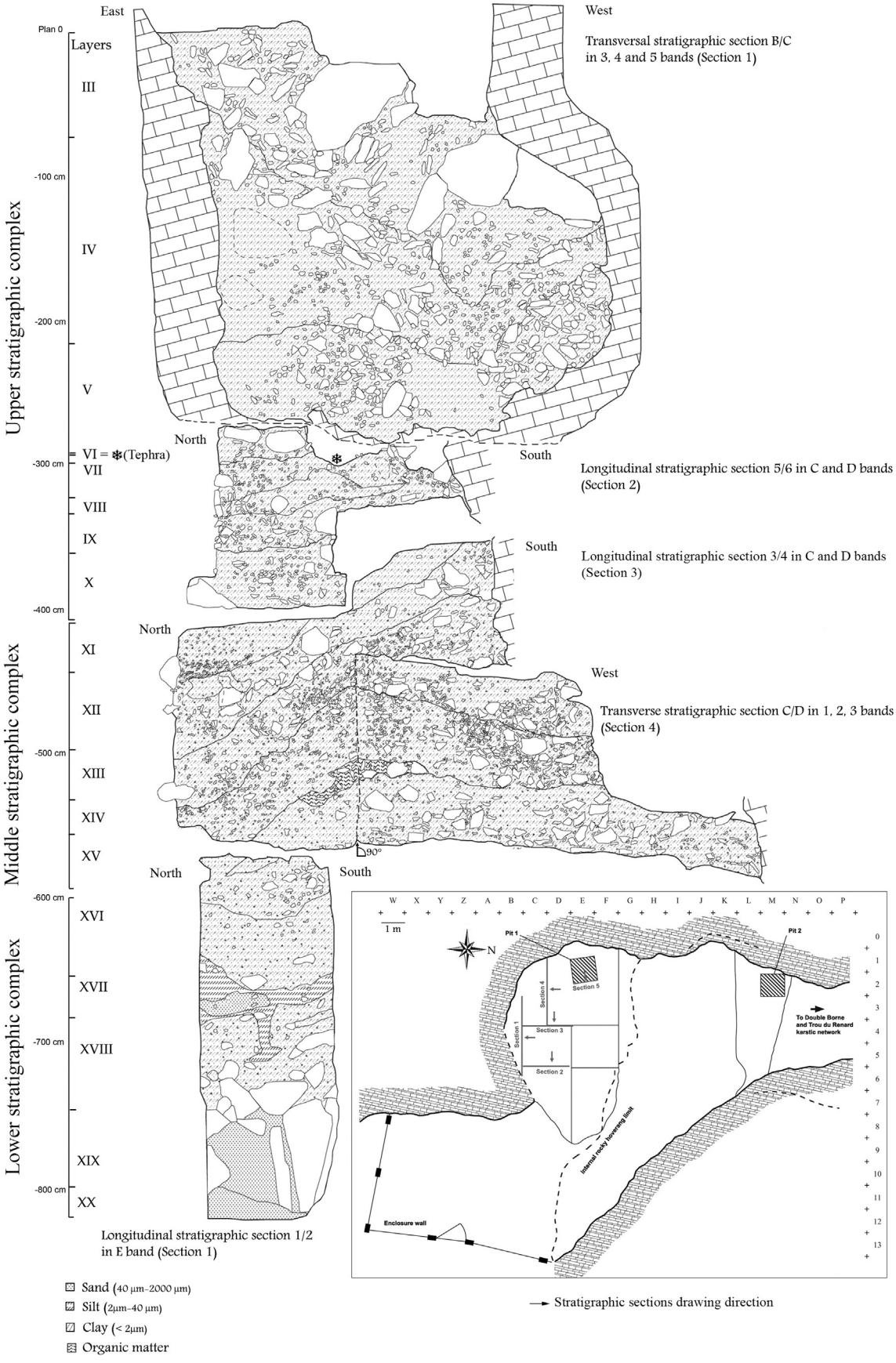

Fig. 2. Stratigraphy of Moula-Guercy and locations of the cross sections (modified from Saos et al., 2014).

The sedimentological sequence can be interpreted as follows: the lower complex represents an active karst system with alluvial deposits from sands to small limestone pebbles. The sediments indicate a cold climate (Saos et al., 2014). With the onset of the deposition of the middle stratigraphic complex, the cave opened to the outside. During this time the cave dried out and the infill is characterised by cave wall fragments and the matrix is dominated by windblown sediments. Importantly, the cave becomes inhabited by animals and men. The sediments indicate a warmer climatic phase. Finally, the upper sedimentological complex shows solifluction in a periglacial environment (Saos et al., 2014).

1.3. Lithics

The more recent excavations yielded a total of 2595 lithic artefacts from 11 layers, 1294 of which were larger than 25 mm (Defleur, 2015). The vast majority of the lithics, 92.3%, were found in four layers (IV, VIII, XIV and XV). The lithics of layers IV and VIII are technologically and typologically distinct from those of XIV and XV. 225 chips larger than 25 mm and 57 retouched tools were found in layer XV. The débitage belongs to the same family of Levallois/discoidal technology (Bordes, 1961). Over 30% of the lithic materials have been identified to come from ~40 km south of the Rhône River between the municipalities of Meysse and Rochemaure, which contains high quality flint (Defleur, 2015). Due to the significant distance of these sources and the use of small flint pebbles and siliceous limestone from the alluvium of the Rhône river, Levallois débitage is low, but of good quality. The retouched tools are very abundant, representing >27% of the total débitage. Almost all of the Levallois flakes were processed into retouched tools or possibly were introduced into the cavity in the form of retouched tools. Levallois core are mainly in imported flint, while discoid nuclei are mostly of materials from the Rhône alluvium. The 57 tools are dominated by simple, transverse and convergent scrapers (Defleur, 2015). At the regional scale lithic assemblages from layer XIV and XV have both typological and technological analogies with Jiboui site in the Vercors dated to MIS 3 (Tillet et al., 2004).

1.4. Biostratigraphy

The climatic phases of the stratigraphic layers can be further investigated using the detailed paleontological studies of macrofauna, microfauna, reptiles and amphibians (Crégut-Bonnoure et al., 2010; Defleur et al., 2001, 2014; Desclaux and Defleur, 1997; Manzano, 2015).

The lower stratigraphic complex does not contain any macrofauna, but a large number of micromammal remains (*Dicrostonyx torquatus*, *Microtus gregalis*, *Sicista betulina*), indicating cold, steppe environmental conditions.

The middle stratigraphic complex is a thick homogenous deposit and contains diverse faunal remains. Layers XIV and XV contain cultural remains including a lithic assemblage, fireplaces, charcoal and abundant fauna such as red deer (*Cervus elaphus*), alpine ibex (*Capra ibex*), fallow deer (*Dama* sp.), straight-tusked elephant (*Palaeoloxodon antiquus*), rhinoceros (*Dicerorhinus hemitoechus*) and many carnivores. Layers XIV to XII contain wolf (*Canis lupus*) remains that are intermediate between Late and Middle Pleistocene. Furthermore, the bear lineage *deningeri-spelaeus* is dominated by the more primitive character of *Ursus deningeri*, the presence of *Ursus thibetanus* in association with brown bear (*Ursus arctos*), badger (*Meles meles*) and wildcat (*Felis silvestris*) is similar to other interglacial sites (Crégut-Bonnoure et al., 2010).

The upper stratigraphic complex contains woolly mammoth (*Mammuthus primigenius*), reindeer (*Rangifer tarandus*), lemming (*Dicrostonyx torquatus*), and vole (*Microtus* (*Stenocranius*) *gregalis*), which also indicates a cold phase. In addition, these layers contain wolf remains whose evolutionary stage is typical for the Upper Pleistocene, as well as bear, hyena and red deer (*Cervus elaphus*) species typical for Upper Pleistocene sites in the southeast of France.

1.5. Chronology

Thermoluminescence dating on quartz from layer VI provided an age of 72 ± 12 ka (Sanzelle et al., 2000). This was used to correlate this tephra layer with two other volcanos in the Ardèche: le Ray-Pic with TL dating on plagioclases: 77 ± 10 ka and/or le Pic de l'Etoile with TL dating on plagioclases: 83 ± 9 ka (Guérin and Gillot, 2007; Guérin, 1983). The first one is characterised by abundant occurrence of basement olivines and shows a strong mineralogical similarity with those found at Moula-Guercy (Debard and Pastre, 2008). Based on the environmental deductions from the sedimentology and biostratigraphy the remaining layers can be placed into the general biochronology of Europe (Crégut-Bonnoure et al., 2010; Defleur et al., 2001; Desclaux et al., 2000). This preliminary assignment broadly places the lower stratigraphic complex to MIS 6, the middle stratigraphic complex MIS 5 and the upper stratigraphic complex to MIS 4. The Neanderthal remains are associated with layer XV in the middle stratigraphic complex. The fauna of layer XV shows the first occurrence of fallow deer and its other faunal elements, such as Hermann's tortoise (*Testudo hermanni*), may be correlated to MIS 5e interglacial sites in the Mediterranean area. The presence of *Hystrix* cf. *vinogradovi*, in association with three species typical of the Middle Pleistocene (*Allocricetus bursae*, *Pliomys lenki* and *Microtus* (*Iberomys*) *brecciensis*) not encountered in association with any late Pleistocene layers in Mediterranean Europe so far, further points towards MIS 5e. A recent study on amphibians and reptiles provides additional support to this chronological attribution (Manzano, 2015). Furthermore, the marked persistence of taxa characteristics of a continental climate and an open environment, such as *Marmota marmota*, *Microtus* (*Stenocranius*) *gregalis* and *Spermophilus citellus*, suggests that this layer is contemporary of the start of the late Pleistocene temperate climatic oscillation.

2. Materials and methods

2.1. Radiocarbon analysis

Accelerator Mass Spectrometry (AMS) radiocarbon dating of five faunal bone samples [M93-C4-IV 21, 22, 26, 32 and M93-C3-IV 28] from layer IV was carried out at the Oxford Radiocarbon Accelerator Unit (ORAU), University of Oxford (Table 1). Prior to dating, the material was subjected to %N testing as a way of assessing the preservation of protein in the bone (Brock et al., 2010b). Two of the Moula-Guercy bones (21 and 28) failed to provide N above the cut-off limit of the ORAU and were not treated further. Three samples were dated using the latest preparation protocol for bone collagen, which includes an ultrafiltration step (Brock et al., 2010a; Higham et al., 2006). About 600 mg of bone powder was drilled from each sample, and collagen was extracted using a series of chemical steps. These steps included immersion in HCl and NaOH for the demineralization and removal of humic acids, respectively, interspersed with cleaning in ultrapure MilliQ water. The extracted collagen was gelatinised and underwent ultrafiltration, after which ~1 ml of >30 kD gelatine was lyophilised. About 5 mg of dried collagen was combusted using a GC–MS system and the CO_2 generated via this process was purified, graphitised, and pressed into target holders prior to its introduction to the AMS system for ^{14}C measurement.

2.2. $^{40}Ar/^{39}Ar$ dating

A sample from the tephra, layer VI, was collected for $^{40}Ar/^{39}Ar$ dating. The $^{40}Ar/^{39}Ar$ dating for sanidine grains followed the protocol of Michel et al. (2013). The largest possible well-preserved sanidine grains (500 μm) were extracted using standard heavy liquid methods and then hand-picked under a binocular microscope. Grains were treated with HNO_3 and HF for 10 min, followed by deionised water for 10 min in an ultrasonic bath. Their chemical composition was estimated using

Table 1
Radiocarbon results from layer IV.

Sample	Material	OxA	^{14}C age BP	Chemistry parameters of dated samples					
				Used bone (mg)	Collagen Yield (mg)	Collagen yield, %	δ^{13}C	δ^{15}N	C:N
M93 C4 IV 21	bone	*Failed*							
M93 C4 IV 22	bone	28,093	>47,000	610	29.69	4.9	-21.2	2.35	3.38
M93 C4 IV 26	bone	28,094	>48,500	600	16.8	2.8	-20.0	5.91	3.38
M93 C4 IV 26	bone	28,095	>48,000	600	17.93	3.0	-20.0	5.78	3.34
M93 C4 IV 32	bone	28,096	>49,400	600	19.99	3.3	-20.6	1.72	3.32
M93 C3 IV 28	bone	*Failed*							

scanning electron microscopy with Energy Dispersive X-ray Spectroscopy (EDS) in order to check the homogeneous presence of potassium (Ecole des Mines, Sophia Antipolis, Valbonne, France). The samples were irradiated for one hour with Cd shielding in 5C position at McMaster University Reactor (Hamilton, Canada). The sanidine grains were subsequently loaded onto a copper plate by sets of about 50–100 grains per hole for multigrain aliquot analyses. Gas was extracted with an infrared continuous laser and purified in stainless and glass extraction line using two Al—Zr getters and a N_2 cold trap. System blanks were run for every two or three analysed samples. The mass spectrometer is a VG3600 with a Daly detector. Mass discrimination was monitored by regularly analysing one air pipette volume. The ultimate accuracy of the ^{40}Ar/^{39}Ar method depends on well-dated homogeneous standards (Nomade et al., 2005).

2.3. Tooth samples

Teeth were selected from the collection in the Musée Archéologique de Soyons. All samples were originally collected *in situ* and were completely cleaned. Combined U-series/ESR dating was carried out on 14 faunal teeth (Fig. 3) and their sample layers are given in Tables 2 and 3. U-series dating was carried out on Neanderthal teeth from layer XV. Tooth 3524 (M-D1–230), Fig. 4A, was intact, while sample 3525 (M-*H*3–73), Fig. 5A, was a tooth fragment. In addition, we analysed one intact tooth (3526) of a Neolithic individual from a grave dug into the uppermost layer, Fig. 6A.

2.4. U-series analysis

The laser ablation U-series analysis was carried out at the Research School of Earth Sciences (RSES), using a custom-built laser ablation sampling system (ANU HelEx) interfaced between an ArF Excimer laser (193 nm; Lambda Physik Compex 110) and a Neptune MC-ICP-MS. Details of the laser ablation system including detailed description of the equipment, sampling strategies, and data reduction, has been given by Grün et al. (2014). U-series analysis on the Neanderthal tooth 3524 and of the Neolithic tooth utilised laser drilling (Benson et al., 2013). Neanderthal tooth 3525 was already broken and analyses were carried out on cross section through the dentine. The faunal samples were cut and analysed along cross sections using laser spot analysis (e.g., Storm et al., 2013). The U concentrations in enamel were too low for U-series isotopic analysis.

2.5. ESR analysis

In order to obtain external dose rate data, *in situ* gamma spectrometric measurements were carried out at the site and representative sediment samples were collected and analysed for U, Th, and K by solution ICP-MS/OES (Genalysis, Perth).

The dating procedures followed those routinely applied in the ANU ESR dating laboratory (Grün et al., 2008). From each faunal tooth, an enamel fragment was removed and powdered. The sample was then successively irradiated in 9 steps to 810 Gy using an X-ray source,

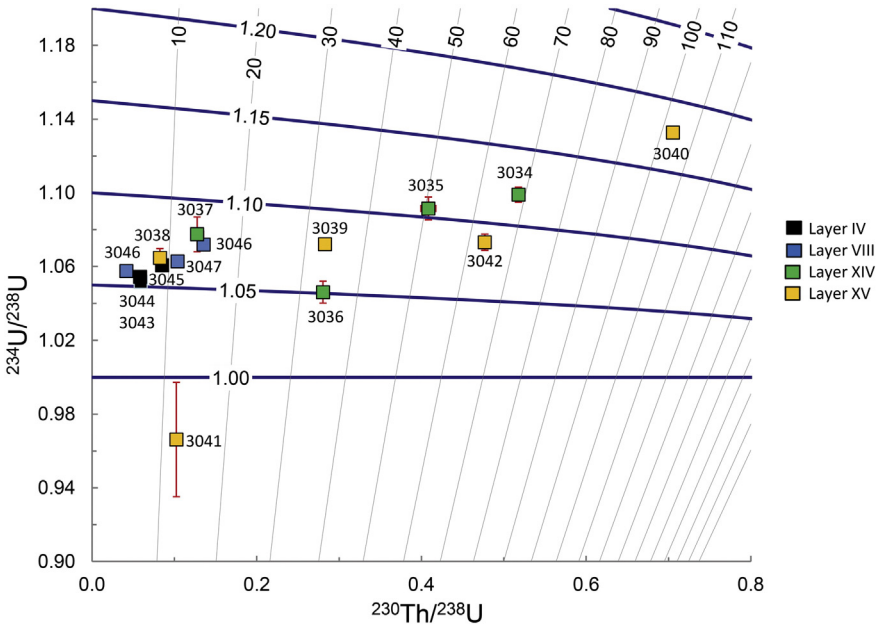

Fig. 3. U-series results of the faunal teeth. Errors are 2σ, plot created using Isoplot (Ludwig, 2003). Solid purple lines highlight the different ^{234}U/^{238}U ratios.

Table 2
U-series results on the faunal teeth from Moula-Guercy. EN stands for enamel and DE for dentine.

Lab number	Field Number	Layer	U(EN) (ppm)	U(DE) (ppm)	U(CE) (ppm)	$^{234}U/^{238}U$ (DE)	$^{230}Th/^{234}U$ (DE)	Apparent age (ka)
3043	M93-F4-29	IV	0.05	33.0		1.0517 ± 0.0022	0.0561 ± 0.0012	6.3 ± 0.1
3044	M93-F5-17	IV	0.15	21.5		1.0544 ± 0.0028	0.0553 ± 0.0015	6.2 ± 0.2
3045	M93-C3-M1	IV	0.09	58.1		1.0607 ± 0.0018	0.0802 ± 0.0010	9.1 ± 0.1
3046	M94-D4-23	VIII	0.75	41.9		1.0576 ± 0.0025	0.0394 ± 0.0009	4.4 ± 0.1
3046					70.0	1.0719 ± 0.0018	0.1265 ± 0.0011	14.7 ± 0.1
3047	M94-C3-222	VIII	0.10	55.1		1.0628 ± 0.0023	0.0977 ± 0.0013	11.2 ± 0.2
3034	M95-D2-154	XIV	0.10	13.8		1.0990 ± 0.0040	0.4712 ± 0.0060	68.8 ± 1.3
3035	M95-D2-287	XIV	0.05	6.1		1.0915 ± 0.0062	0.3742 ± 0.0080	50.8 ± 1.5
3036	M95-G2-46	XIV	0.05	8.6		1.0461 ± 0.0060	0.2681 ± 0.0069	34.0 ± 0.9
3037	M95-G2-83	XIV	0.07	2.2		1.0775 ± 0.0094	0.1184 ± 0.0071	13.7 ± 0.9
3038	M95-F3-217	XV	0.03	7.6		1.0647 ± 0.0051	0.0774 ± 0.0036	8.8 ± 0.4
3039	M97-784	XV	0.14	22.5		1.0721 ± 0.0030	0.2638 ± 0.0037	33.3 ± 0.6
3040	M95-F2	XV	0.18	25.3		1.1327 ± 0.0023	0.6227 ± 0.0042	103.7 ± 1.4
3041	M97-F1-398	XV	0.30	57.2		0.9662 ± 0.0310	0.1060 ± 0.0015	12.2 ± 0.2
3042	M06-96-E1-177	XV	0.01	9.6		1.0732 ± 0.0044	0.4444 ± 0.0059	63.7 ± 1.1

which was calibrated using secondary standards (samples that had previously been irradiated with a calibrated gamma source).

For the calculation of the internal dose rate values we used beta attenuation values of Marsh (1999) and an alpha efficiency of 0.13 ± 0.02 (Grün and Katzenberger-Apel, 1994). Dose rates were calculated with the conversion factors of Guérin et al. (2011). For the estimation of the cosmic dose rate (Prescott and Hutton, 1988) a mean depth of 10 ± 5 m was assumed, to account for the changes in overlaying sediment thicknesses through time, resulting in consistent cosmic dose rates as reported in Sanzelle et al. (2000). For layer XV, gamma dose rate measurements were carried out by thermoluminescent dosimeters (TLDs) by Helene Valladas in 1993. Due to the low thickness of layer XV and high occurrence of lithic artefacts TLDs could only be inserted in limited places, and to better reflect the overall gamma dose rate, all six measurements were averaged. A time averaged water content of 10 ± 5% was assumed for the sediments and dentine. The U concentrations in enamel were too low for U-series isotopic analysis. For the calculation of the enamel dose rates the dentine U-series values were used. Age calculations were carried out with the ESR-DATA program (Grün, 2009) for combined U-series/ESR (Grün et al., 1988) and the closed system U-series (CSUS) ESR system (Grün, 2000).

3. Results and discussion

3.1. Radiocarbon dating

The dating results are summarised in Table 1. One bone sample (26) was dated twice (OxA-28,094 and OxA-28,095) as a routine internal laboratory check. Both results were infinite - greater than background ages, as were the two further determinations (OxA-28,093 and OxA-28,096). These ages provide a minimum age for the formation of layer IV, which predates 50 ka BP.

3.2. $^{40}Ar/^{39}Ar$ dating

Each laser step-heating experiment of the multigrain aliquots from the tephra of layer VI provided an extremely high ^{40}Ar signal (>6 V) whereas the ^{39}Ar signal was very low (under 15 mV), suggesting that these sanidines are not of Quaternary age. The estimated ages are older than 200 Ma. Thus, the new $^{40}Ar/^{39}Ar$ dating results unfortunately did not provide any tangible chronological information and are excluded from the further discussion on the chronology of Moula-Guercy.

3.3. U-series on faunal teeth

For the interpretation of the U-series data one has to keep in mind that the U-series ages are indications of when uranium migrated into the skeletal tissue. Firstly, there can be a long delay between the deposition of a bone or tooth and the U-uptake. Secondly, there may be several consecutive overprinting uptake phases in the skeletal tissue (see e.g., Grün et al. (2014), and sample 3525, below). Thus, apparent U-series ages have generally to be regarded as minimum age estimates. However, U migration processes can be highly complex and U-leaching can also occur, leading to older apparent ages. Leaching is usually associated with lower U-concentrations in the effected domains compared to their surroundings.

The U-series results on the faunal teeth are given in Table 2 and shown in Fig. 3. For layer IV, all apparent U-series determinations are of Holocene age, whereas for layer VIII, of late Pleistocene to early Holocene age. The results from layer XIV vary between around 14 and 70 ka and those of layer XV between 9 and 104 ka. Since the sedimentological and biochronological data of this cave indicate that these layers are in stratigraphic order (Defleur et al., 2014; Saos et al., 2014) we attribute the huge spread in U-series age results from the faunal teeth to be caused by complex U-migration on small scales. In an intact sample the $^{234}U/^{238}U$ ratios change little within a tooth and are an indication of the U source. As it can be seen, layer IV has very similar $^{234}U/^{238}U$ ratios, but with the increase in age spread in the lower layers the spread in $^{234}U/^{238}U$ ratios also increase. That is a sign that the U sources for the different teeth were different, most probably by the position within a given layer. Samples 3040 and 3041 have distinct $^{234}U/^{238}U$ ratios from all other samples. It is important to note that in spite of having very different U-series isotopic compositions, none of the samples

Table 3
Sediment data for ESR dating.

Layer	U (ppm)	Th (ppm)	K (ppm)	External Gamma dose rate (μGy/a)	Cosmic dose rate (μGy/a)
IV	3.53 ± 0.18	9.80 ± 0.49	8904 ± 1000	581 ± 25	63 ± 23
VIII	3.46 ± 0.17	9.13 ± 0.46	11,800 ± 1000	546 ± 25	63 ± 23
XIV	3.68 ± 0.18	10.70 ± 0.54	14,800 ± 1000	709 ± 41	63 ± 23
XV	4.55 ± 0.22	9.39 ± 0.47	16,700 ± 1000	642 ± 98	63 ± 23

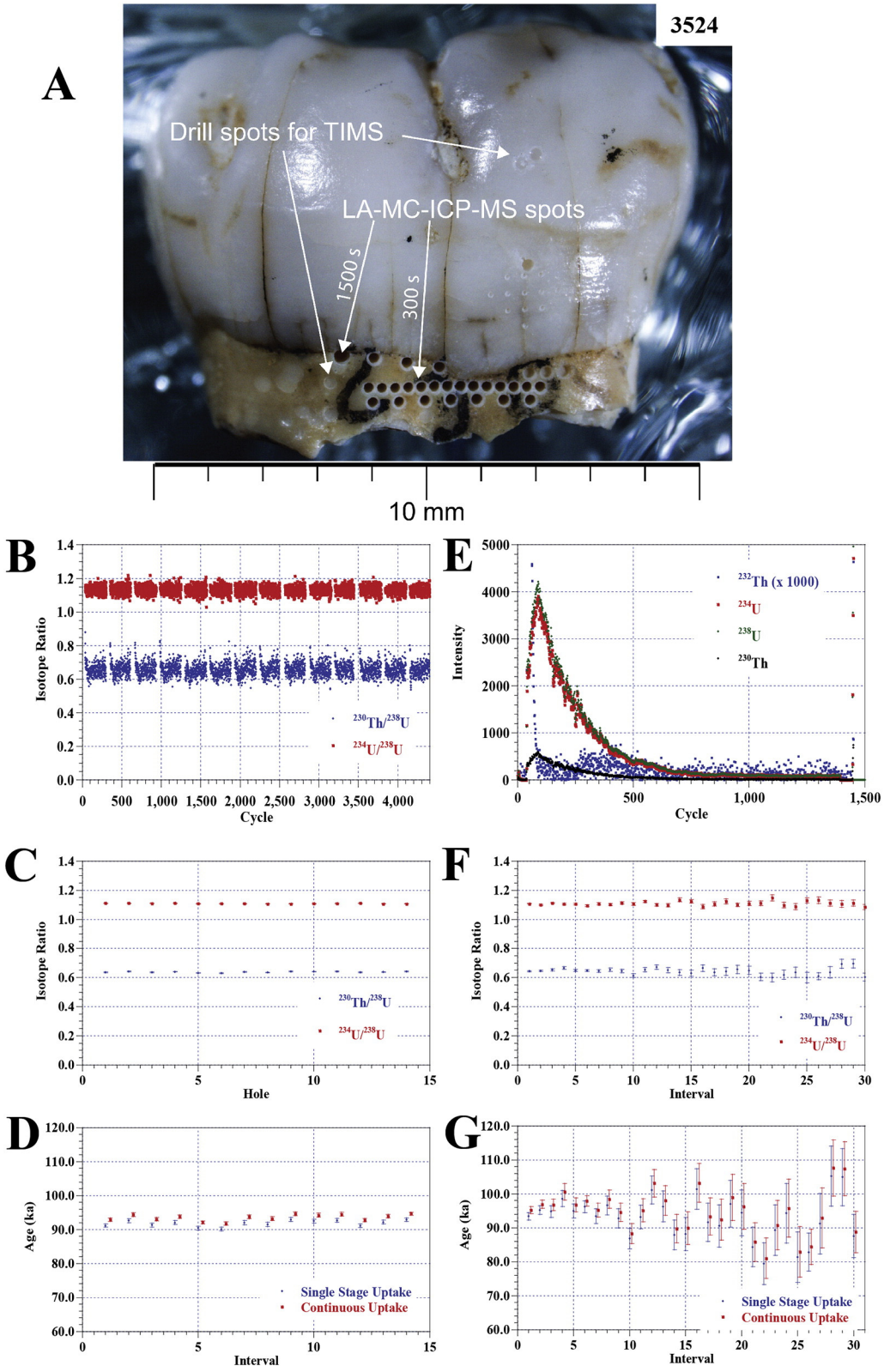

Fig. 4. U-series results of Neanderthal tooth 3524. (A) Photo and location of the sampling spots from LA-MC-ICP-MS and TIMS (Benson et al., 2013). (B) U-series isotope ratios along the 300 s drill holes. (C) Binned data of B. (D) Apparent U-series ages for closed system (single stage uptake) and continuous diffusion from B. (E) Isotope measurements along the 1500 s drill hole. (F) Binned isotope ratios. (G) Apparent U-series ages for closed system (single stage uptake) and continuous diffusion from E.

show any indication of U-leaching. The U-series results on faunal materials from various layers demonstrate a greatly delayed U-uptake yielding results which are significantly younger than the expected ages from biostratigraphy. The data on the faunal teeth show that U-series on bones and teeth alone can lead to considerable age underestimations.

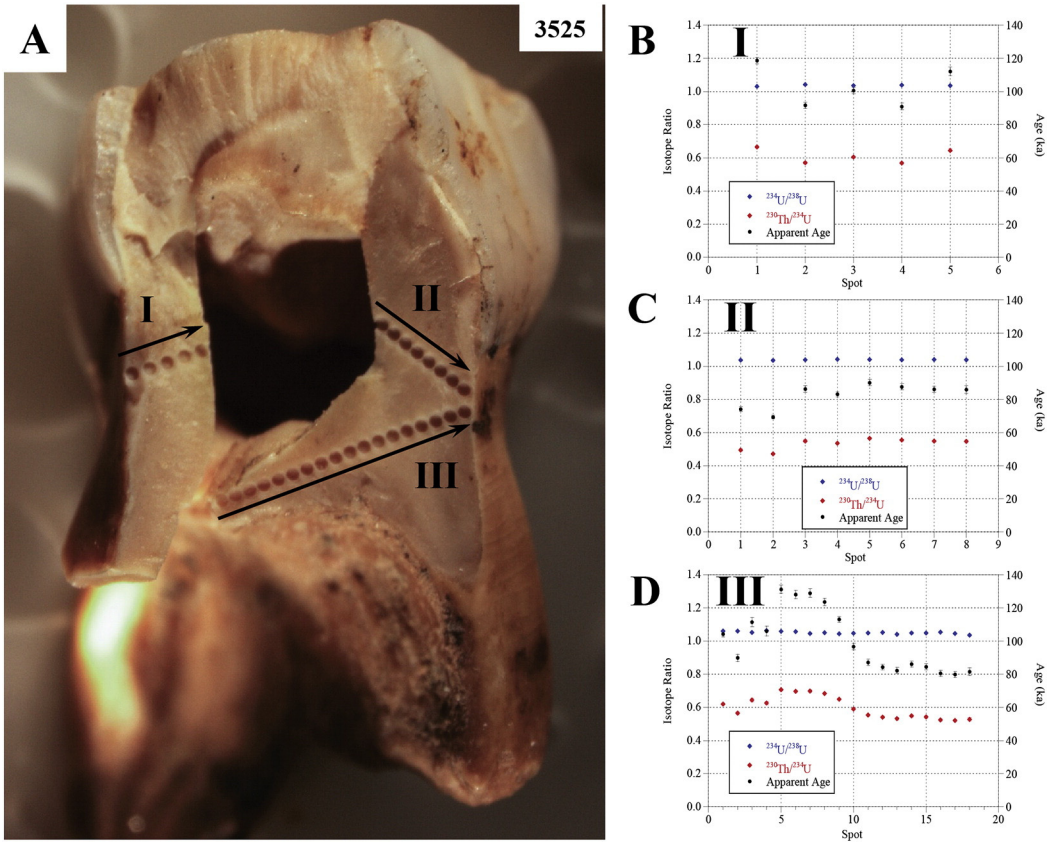

Fig. 5. U-series results of Neanderthal tooth 3525. (A) Photo and location of the transects. (B) Isotope ratios and apparent U-series age estimates along transect I. (C) Isotope ratios and apparent U-series age estimates along transect II. (D) Isotope ratios, U-concentrations and apparent U-series age estimates along transect III.

3.4. U-series on human teeth

Neanderthal tooth 3524 (Fig. 4) was analysed using laser ablation scans of 14 holes (Fig. 4B) and a 1500s hole (Fig. 4E). The results of the 14 holes (Fig. 4D) yield mean age of 91.8 ± 0.9 ka, each age estimation has a mean error of 0.55 ka. This shows that there is some inhomogeneity in the U-series composition within the range of the 14 holes. The 1500s scan was binned into 30 sections with a length of 40 cycles. It is clearly visible that the errors in the isotope ratios (Fig. 4F) and consequently the calculated ages (Fig. 4G) increase as the isotope intensities decrease (Fig. 4E). Nevertheless, the mean of the 30 age calculations along the depth probing 92.8 ± 6.3 ka is indistinguishable from the previous measurements. The mean errors increased nearly tenfold to 4.9 ka. Using the continuous diffusion model for uranium acquisition of Sambridge et al. (2012), the ages become slightly older, but only by about 1.8 ka (see Fig. 4D,G).

The results of sample 3525 show the full complexity of U-migration into teeth (Fig. 5). As it was a broken specimen, we could measure several transects through various dentine sections. The results of all three sections are different. Transect I (Fig. 5B) yielded ages between 90 and 120 ka, and it is possible to calculate an age using the diffusion-adsorption-decay (DAD) model of Sambridge et al. (2012), yielding an age of 118 ± 15 ka (2σ). The first two spots of transect II (Fig. 5C) yielded younger ages of around 70 ka while the rest yielded ages of around 86 ka. Transect III (Fig. 5D) starts with ages of around 95 ka, increasing to around 130 ka (spots 5 to 7) then decreasing back to around 82 ka towards the outside of the tooth. This shows that even small teeth may experience complex U-uptake histories. Contrary to expectations, the high age values in transect III are associated with higher U-concentrations, i.e. it is unlikely that the older ages were the result of U-leaching. It seems that there is an earlier U-uptake phase from the base of the tooth, perhaps around 120 to 130 ka migrating from the lower end into the dentine as well as from the left side (as in the photo) followed by diffusion from the right side and somewhat later overprinted near the pulp cavity. The U-series analyses of the two Neanderthal teeth demonstrate that layer XV at least corresponds to MIS 5 *sensu lato*. As all results still have to be regarded as minimum age estimates, any older age cannot be excluded: the results of the faunal teeth of layer IV indicate a delay in U-uptake of at least 45 ka.

The tooth of the Neolithic individual yielded only one analysis that could be evaluated (Fig. 6). Cycles 1 to 20 and 21 to 40 yield ages of 4.8 ± 1.4 ka and 3.6 ± 1.6 ka, respectively. However, the mean ^{230}Th is generally only 1.1 and 0.6 counts above background, which was 1.4 counts per cycle, i.e., any age results are critically dependent on the accurate assessment of the background levels. The very low U-concentrations in this tooth may be taken as indication that U-accumulation was delayed in the other human teeth as well.

The U-uptake into skeletal elements recovered from the sediments of Moula-Guercy involves complex processes, and even small human teeth are subject to complicated U-migration histories.

3.5. ESR dating on faunal teeth

For ESR dating of teeth an assessment of the dose rates of the surrounding sediments is critical. All samples had been cleaned long before the measurement of the dose rates of the sediment layers. The U, Th and K contents, gamma dose rates and cosmic dose are listed in Table 3. The external gamma dose rates in layer XV, where six independent measurements were carried out, vary between 500 μGy/a, and 733 μGy/a. This implies that the actual external dose rate (beta and gamma) at a given place within a layer could vary by as much 20–40%.

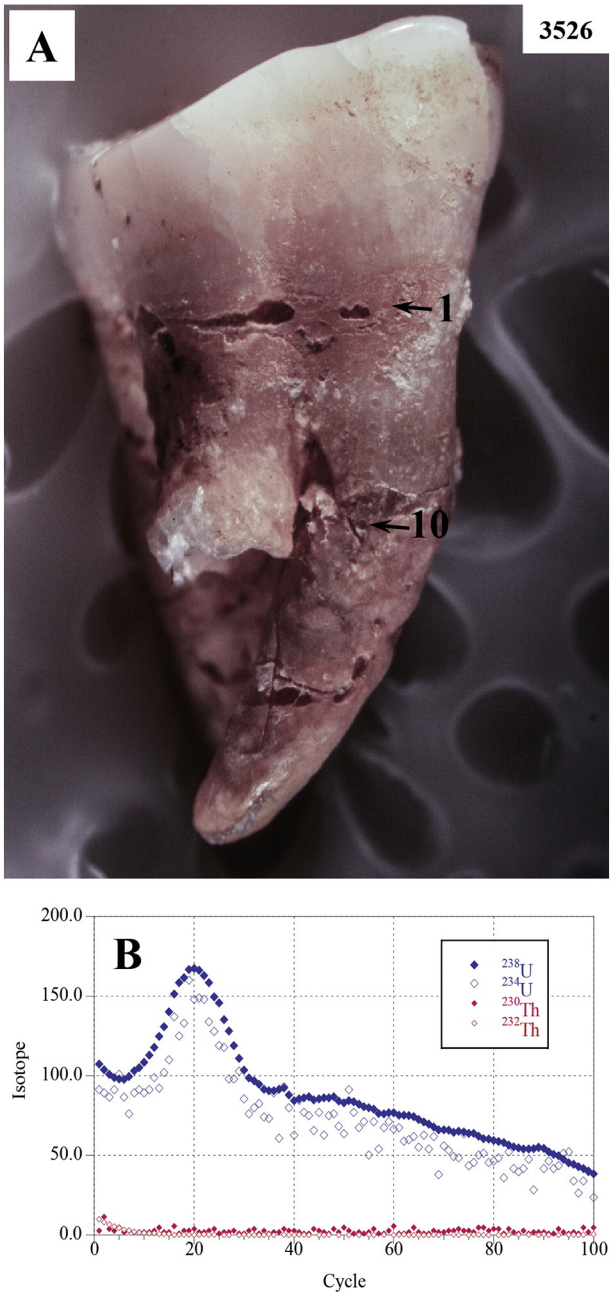

Fig. 6. U-series results of the Neolithic tooth (3526). (A) Photo and location of the laser ablation drill holes. (B) Isotope measurements of the first 100 cycles of hole one.

The results of the ESR measurements and age calculation in Table 4. Since all teeth were analysed for U-series, we present only combined US/ESR (Grün et al., 1988) and CSUS/ESR (Grün, 2000) age calculations. The difference between the models is that the former assumes a continuous U uptake while the latter assumes a single short phase uptake at a time that corresponds to the closed system U-series age. The two models encompass all possible U-uptake scenarios (except for leaching). As it can be seen in Table 4, there is only one sample (3039) where the CSUS/ESR model yielded an 11 ka older age, however, still within overlapping errors. All other results are indistinguishable. All *p*-values indicate a continuous uranium accumulation excepted for the tooth 3040. This sample is suspected to have undergone uranium leaching and consequently is discarded from further analysis.

We note that three teeth (3046, 3037 and 3038), from layer VIII, XIV and XV respectively, returned significantly younger ages than were expected based on the stratigraphy and biostratigraphy of the site and as the other samples from the same layers. Incorporation of these samples from higher layers in the cave is unlikely based on the known intact stratigraphy of the site (Defleur et al., 2014; Saos et al., 2014). All of these younger aged samples have closely similar dose values between 33.7 and 36 Gy, none of the other samples have such low dose values. This indicates that they were located in low dose rate environments (surrounded by large limestone blocks), which is also supported by the field data. These three samples were thus removed from the age interpretation of their corresponding layer.

Detailed studies on the composition of the ESR signals in teeth show that gamma irradiation induced large amounts of unstable components (Joannes-Boyau and Grün, 2011). A sample from Broken Hill in Zambia yielded a 30% higher dose value once the dose response curve was corrected for these unstable components. However, the teeth from Moula-Guercy were irradiated with an X-ray source, which induced significantly less unstable signals, in the range of 6%, of the natural signal (Grün et al., 2012b). In contrast to the U-series results, it is not possible to assume that the oldest ESR results come closest to the age of deposition. The scatter in the ESR ages is in the first instance caused by our inability to accurately reconstruct the external dose rate for a given tooth. It seems that ESR, in spite of all its conceived failings, is essential for reconstructing chronologies for complex sites, such as Moula-Guercy. The newly developed dating procedures using laser ablation drilling will help to tighten the ages of human fossils, however, additional analyses seem essential to move from minimum U-series age estimates to more constrained age assessments. It has to be noted that nearly non-destructive ESR analysis, which also allows the quantification of thermally unstable components, is a highly work intensive process (Joannes-Boyau and Grün, 2011, and references therein). Furthermore, the tendency of palaeoanthropologists to CT scan everything that comes out of excavations will make direct ESR dating of human teeth virtually impossible (Grün et al., 2012a).

Table 4
ESR results, EN stands for enamel and DE for dentine. Samples in parentheses were not used for the age interpretation for that layer.

Lab number	Layer	D_e (Gy)	TT (μm)	EN + DE DR (μGy/a)	Beta SED (μGy/a)	Total DR (μGy/a)	*p*-value (DE)	US/ESR Age (ka)	CSUS/ESR Age (ka)
3043	IV	44.7 ± 0.8	900	31 ± 5	180 ± 25	856 ± 41	6.08 ± 0.45	52 ± 2	52 ± 2
3044	IV	50.9 ± 0.8	1050	16 ± 2	157 ± 21	817 ± 39	7.77 ± 0.58	62 ± 3	62 ± 3
3045	IV	60.3 ± 1.1	1000	58 ± 10	164 ± 22	867 ± 40	5.36 ± 0.41	69 ± 4	69 ± 3
3046	VIII	36.0 ± 0.6		32 ± 3		787 ± 43	8.22 ± 0.70	45 ± 3	(46 ± 2)
3047	VIII	56.4 ± 1.0	1100	68 ± 11	170 ± 22	847 ± 41	3.70 ± 0.32	66 ± 4	66 ± 4
3034	XIV	n/a							
3035	XIV	98.1 ± 2.1	1100	35 ± 6	201 ± 36	1008 ± 59	0.23 ± 0.11	97 ± 7	97 ± 6
3036	XIV	73.9 ± 1.4	950	42 ± 9	230 ± 46	1045 ± 64	0.04 ± 0.13	70 ± 5	70 ± 4
3037	XIV	33.7 ± 0.8	1350	9 ± 2	165 ± 24	946 ± 52	0.51 ± 0.21	35 ± 2	(35 ± 2)
3038	XV	34.7 ± 0.6	1200	13 ± 3	226 ± 40	944 ± 107	2.07 ± 0.55	36 ± 5	(36 ± 4)
3039	XV	109.8 ± 2.5	1050	72 ± 14	236 ± 30	1013 ± 105	0.98 ± 0.35	108 + 15/−11	119 ± 13
3040	XV	109.1 ± 2.1	1000	no US/ESR	calculation	Possible	U-series	too old	
3041	XV	120.8 ± 3.0	950	52 ± 11	259 ± 34	1016 ± 106	7.26 ± 1.14	118 + 16/−12	119 ± 13
3042	XV	101.2 ± 2.1	900	71 ± 14	272 ± 37	1049 ± 110	0.58 ± 0.015	96 + 13/−9	97 ± 10

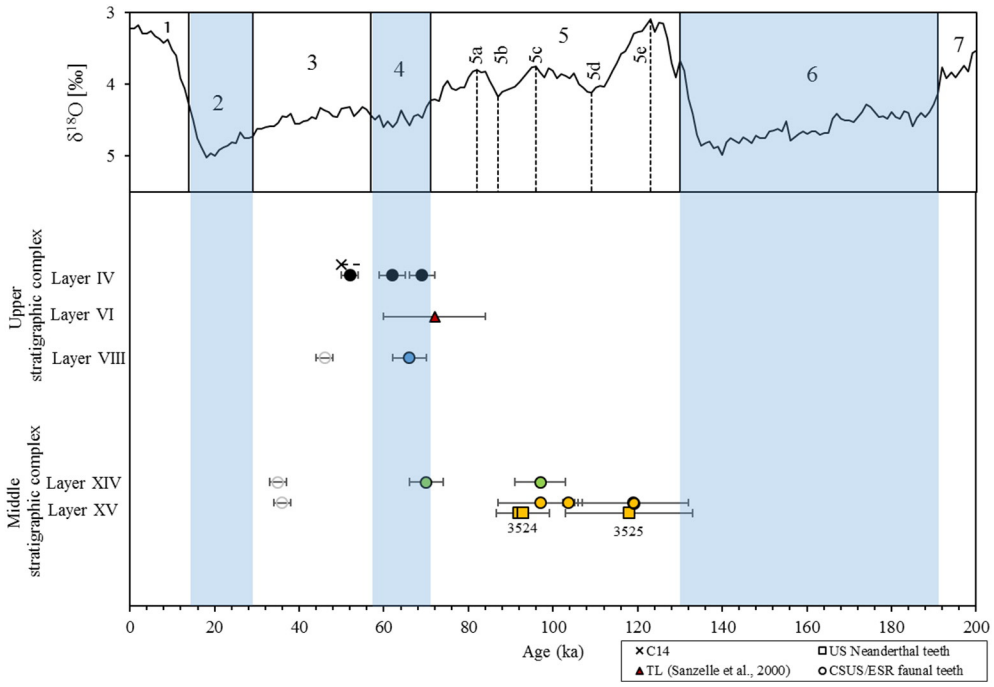

Fig. 7. Summary of the refined chronology of Moula-Guercy. $\delta^{18}O$ data for the last 200 ka is the LR04 stack of marine benthic foraminiferal of Lisiecki and Raymo (2005). Marine isotope stage boundaries and sub-stage peaks (Lisiecki and Raymo, 2005; Shackleton, 1969) are shown, with blue colours indicating cold climatic conditions. Grey, hollow circles are samples with unusually low dose rates, excluded from age estimation for their corresponding layer. (For interpretation of the references to colour in this figure legend, the reader is referred to the web version of this article.)

3.6. Chronology of Moula-Guercy

This study provides the first comprehensive chronology of Moula-Guercy (Fig. 7). The radiocarbon dating results on bone samples show that layer IV is older than 50 ka. Combined CSUS/ESR results on three faunal teeth (3043, 3044, 3045) from the same layer yielded age estimates, ranging from 52 ± 2 ka to 69 ± 3 ka, consistent with the radiocarbon results. This places layer IV at the end of MIS 3 to MIS 4 (Fig. 7), in agreement with the age of the TL dating on layer VI, located just below, with an age of 72 ± 12 ka (Sanzelle et al., 2000). For layer VIII only two faunal teeth (3046, 3047) were analysed and one sample (3046) was excluded because it was located in a low dose rate environment (see discussion 3.5). With only one sample we tentatively place this layer at 66 ± 4 ka, corresponding to the end of MIS 4. The CSUS/ESR ages for layer XIV ($n = 2$) are not conclusive, with one age estimate at 70 ± 4 ka and another at 97 ± 6 ka. The younger age estimation for layer XIV does not agree with the stratigraphy and biostratigraphy of the site and more direct dating of material from this layer is needed to resolve this discrepancy. The age estimates of the Neanderthal fossil bearing layer XV are based on 3 faunal teeth (3039, 3041, 3042), yielding consistent ESR age estimates ranging between 97 ± 10 ka and 119 ± 13 ka. This layer corresponds to the later stages of MIS 5, and is younger than MIS 6 (Fig. 7), in agreement with the climatological and chronological deductions from the stratigraphy and biostratigraphy of the site. The difference in age estimates for the younger age of layer XIV and the age range of XV are unexpected, since these layers are only distinguished by the presence of human remains. Micro and macro fauna, as well as lithics in these layers are similar (Defleur, 2015). Direct U-series analyses on two Neanderthal teeth agree with an age for layer XV corresponding to at least MIS 5 *sensu lato*. The U-series results on the Neanderthal tooth 3525 show that U-mobilisation even into small teeth is highly complex, but nevertheless give an indication that this sample corresponds to MIS 5e. If layer XV was accumulated within a reasonably short time range, as proposed in Saos et al. (2014), its minimum age would be given by the U-series results from 3524 and the upper age range from transect III in 3525, i.e. around 120–130 ka. However, it would be difficult to assess a maximum age, because U-series results on bone and tooth material are considered a minimum age. This is best illustrated by the Neolithic tooth, where large domains did not experience any U-uptake.

The chronology established in this study corroborates the existing stratigraphic and biostratigraphic framework. Moula-Guercy now stands as a reference site for the understanding of this particular aspect of human behaviour.

Acknowledgements

We are grateful to Hélène Valladas, for providing the dose rate data on layer XV. We thank the musée archéologique de Soyons for access to the sample collections. We also extend our thanks to Sylvain Gallet and Chrystèle Vérati (Géoazur), and M. Duval (CENIEH) for helpful discussions. We thank the editor and an anonymous reviewer for valuable comments that greatly improved the quality of this manuscript. The study was funded by the CEPAM, UMR7264-CNRS and by Géoazur (26066/NM/VM/BQR), UMR7329-CNRS. Aspects of this study were funded through ARC Discovery grant DP110101415 *Understanding the migrations of prehistoric populations through direct dating and isotopic tracking of their mobility patterns* (Grün, Spriggs, Armstrong, Maureille, Falgueres).

References

Benson, A., Kinsley, L., Willmes, M., Defleur, A., Kokkonen, H., Mussi, M., Grün, R., 2013. Laser ablation depth profiling of U-series and Sr isotopes in human fossils. J. Archaeol. Sci. 40, 2991–3000. http://dx.doi.org/10.1016/j.jas.2013.02.028.

Bordes, F., 1961. Typologie du paléolithique ancien et moyen. Publications de l'Institut de Préhistoire de l'Université de Bordeaux, Bordeaux. Delmas, p. 2.

Brock, F., Higham, T., Ditchfield, P., Ramsey, C.B., 2010a. Current pretreatment methods for AMS radiocarbon dating at the Oxford radiocarbon accelerator unit (ORAU). Radiocarbon 52, 103–112. http://dx.doi.org/10.2458/azu_js_rc.52.3240.

Brock, F., Higham, T., Ramsey, C.B., 2010b. Pre-screening techniques for identification of samples suitable for radiocarbon dating of poorly preserved bones. J. Archaeol. Sci. 37, 855–865. http://dx.doi.org/10.1016/j.jas.2009.11.015.
Crégut-Bonnoure, E., Guérin, C., 1986. La faune de mammifères de l'Abri Moula (Soyons, Ardèche). Bull. la Société d'Étude des Sci. Nat. Vauclus. 2, 41–72.
Crégut-Bonnoure, É., Boulbes, N., Daujeard, C., Fernandez, P., Valensi, P., 2010. Nouvelles données Sur La Grande faune de l'Émien dans le Sud-Est de la France. Quaternaire 21, 227–248. http://dx.doi.org/10.4000/quaternaire.5592.
Daujeard, C., Moncel, M.-H., 2010. On Neanderthal subsistence strategies and land use: a regional focus on the Rhone Valley area in southeastern France. J. Anthropol. Archaeol. 29, 368–391. http://dx.doi.org/10.1016/j.jaa.2010.05.002.
Debard, É., Pastre, J.-F., 2008. Nouvelles données sur les téphras pléistocènes piégés dans les remplissages karstiques ardéchois (SE France). Quaternaire 19, 107–116. http://dx.doi.org/10.4000/quaternaire.2362.
Defleur, A., 1989. Le Moustérien de l'abri Moula (Soyons, Ardèche). Bull. Soc. Ét. Seien. Nat Vauclus. 59, 59–85.
Defleur, A., 1999. Neanderthal cannibalism at Moula-Guercy, Ardèche, France. Science 286, 128–131. http://dx.doi.org/10.1126/science.286.5437.128.
Defleur, A., 2015. Les industries lithiques moustériennes de la Baume Moula-Guercy (Soyons, Ardèche). Fouilles 1993–1999. l'Anthropologie 119, 170–253. http://dx.doi.org/10.1016/j.anthro.2015.04.002.
Defleur, A., Dutour, O., Valladas, H., Vandermeersch, B., 1993. Cannibals among the Neanderthals? Nature 362, 214. http://dx.doi.org/10.1038/362214a0.
Defleur, A., Crégut-Bonnoure, É., Desclaux, E., Thinon, M., 2001. Présentation paléoenvironnementale du remplissage de la Baume Moula-Guercy à Soyons (Ardèche): implications paléoclimatiques et chronologiques. l'Anthropologie 105, 369–408. http://dx.doi.org/10.1016/S0003-5521(01)80022-4.
Defleur, A.R., Baillon, S., Black, M.T., Brudvik, K., Carlson, J.P., Condemi, S., Crégut-Bonnoure, E., Desclaux, E., Djerrab, A., Douka, K., Guatelli-Steinberg, D., Guipert, G., Hlusko, L.J., Jabbour, R.S., Krueger, K.L., Longo, L., Manzano, A., Mersey, B., Michel, V., Saos, T., Thinon, M., Ungar, P.S., Valensi, P., J.-L V., 2014. La Baume Moula-Guercy, Soyons. Ardèche, Ministère de la Culture, Lyon (545 p.).
Desclaux, E., Defleur, A., 1997. Étude préliminaire des micromammifères de la Baume Moula-Guercy à Soyons (Ardèche, France). Systématique, biostratigraphie et paléoécologie. Quaternaire 8, 213–223. http://dx.doi.org/10.3406/quate.1997.1574.
Desclaux, E., Abbassi, M., Marquet, J.-C., Chaline, J., Kolfschoten, T.V., 2000. Distribution of Arvicola (Mammalia, Rodentia) in France and Liguria (Italy) during the Middle and Upper Pleistocene. Acta Zool. Cracov. 43, 107–125.
Grün, R., 2000. An alternative for model for open system U-series/ESR age calculations: (closed system U-series)-ESR, CSUS-ESR. Ancient TL 18, 1–4.
Grün, R., 2009. The DATA program for the calculation of ESR age estimates on tooth enamel. Quat. Geochronol. 4, 231–232. http://dx.doi.org/10.1016/j.quageo.2008.12.005.
Grün, R., Katzenberger-Apel, O., 1994. An alpha irradiator for ESR dating. Ancient TL 12, 35–38.
Grün, R., Schwarcz, H.P., Chadam, J., 1988. ESR dating of tooth enamel: coupled correction for U-uptake and U-series disequilibrium. Int. J. Radiat. Appl. Instrum. Part D. Nucl. Tracks Radiat. Meas. 14, 237–241. http://dx.doi.org/10.1016/1359-0189(88)90071-4.
Grün, R., Wells, R., Eggins, S., Spooner, N., Aubert, M., Brown, L., Rhodes, E., 2008. Electron spin resonance dating of South Australian megafauna sites. Aust. J. Earth Sci. 55, 917–935. http://dx.doi.org/10.1080/08120090802097419.
Grün, R., Athreya, S., Raj, R., Patnaik, R., 2012a. ESR response in tooth enamel to high-resolution CT scanning. Archaeol. Anthropol. Sci. 4, 25–28. http://dx.doi.org/10.1007/s12520-011-0079-7.
Grün, R., Mahat, R., Joannes-Boyau, R., 2012b. Ionization efficiencies of alanine dosimeters and tooth enamel irradiated by gamma and X-ray sources. Radiat. Meas. 47, 665–668. http://dx.doi.org/10.1016/j.radmeas.2012.03.018.
Grün, R., Eggins, S., Kinsley, L., Moseley, H., Sambridge, M., 2014. Laser ablation U-series analysis of fossil bones and teeth. Palaeogeogr. Palaeoclimatol. Palaeoecol. 416, 150–167. http://dx.doi.org/10.1016/j.palaeo.2014.07.023.
Guérin, G., 1983. La thermoluminescence des plagioclases, méthode de datation du volcanisme. Application au domaine volcanique français: chaîne des Puys, Mont-Dore et Césallier, Bas-Vivarais. Paris VI University (PhD Thesis).
Guérin, G., Gillot, P.Y., 2007. Nouveaux éléments de chronologie du volcanisme Pléistocène du bas Vivarais (Ardèche, France) par thermoluminescence. Compt. Rendus Geosci. 339, 40–49. http://dx.doi.org/10.1016/j.crte.2006.10.005.
Guérin, G., Mercier, N., Adamiec, G., 2011. Dose-rate conversion factors: update. Ancient TL 29, 5–8.
Higham, T., Jacobi, R., Ramsey, C., 2006. AMS radiocarbon dating of ancient bone using ultrafiltration. Radiocarbon 48, 179–195.
Hijmans, R.J., Cameron, S.E., Parra, J.L., Jones, P.G., Jarvis, A., 2005. Very high resolution interpolated climate surfaces for global land areas. Int. J. Climatol. 25, 1965–1978. http://dx.doi.org/10.1002/joc.1276.
Hlusko, L.J., Carlson, J., Guatelli-Steinberg, D., Krueger, K.L., Mersey, B., Ungar, P.S., Defleur, A., 2013. Neanderthal teeth from Moula-Guercy, Ardeche, France. Am. J. Phys. Anthropol. 151, 477–491. http://dx.doi.org/10.1002/ajpa.22291.
Joannes-Boyau, R., Grün, R., 2011. A comprehensive model for CO2– radicals in fossil tooth enamel: implications for ESR dating. Quat. Geochronol. 6, 82–97. http://dx.doi.org/10.1016/j.quageo.2010.09.001.
Lisiecki, L.E., Raymo, M.E., 2005. A Pliocene-Pleistocene stack of 57 globally distributed benthic δ 18 O records. Paleoceanography 20. http://dx.doi.org/10.1029/2004PA001071.
Ludwig, K.R., 2003. A Geochronological Toolkit for Microsoft Excel: Berkeley Geochronol. Cent. Spec. Publ.
Manzano, A., 2015. Les amphibiens et les reptiles des sites Pléistocène moyen de la France méditerranéenne (Caune de l'Arago, grotte du Lazaret et Baume Moula-Guercy). Etude systématique, Reconstitutions paléoclimatiques et paléoenvironnementales. Université de Perpignan Via Domitia, Perpignan, France (PhD Thesis).
Marsh, R.E., 1999. Beta-gradient isochrons using electron paramagnetic resonance: towards a new dating method in archaeology (MSc Thesis) McMaster University, Hamilton.
Mersey, B., Brudvik, K., Black, M.T., Defleur, A., 2013a. Neanderthal axial and appendicular remains from Moula-Guercy, Ardèche, France. Am. J. Phys. Anthropol. 152, 530–542. http://dx.doi.org/10.1002/ajpa.22388.
Mersey, B., Jabbour, R.S., Brudvik, K., Defleur, A., 2013b. Neanderthal hand and foot remains from Moula-Guercy, Ardèche, France. Am. J. Phys. Anthropol. 152, 516–529. http://dx.doi.org/10.1002/ajpa.22389.
Michel, V., Shen, G., Shen, C.-C., Wu, C.-C., Vérati, C., Gallet, S., Moncel, M.-H., Combier, J., Khatib, S., Manetti, M., 2013. Application of U/Th and 40Ar/39Ar dating to Orgnac 3, a late Acheulean and early middle Palaeolithic site in Ardèche, France. PLoS One 8, e82394. http://dx.doi.org/10.1371/journal.pone.0082394.
Nomade, S., Renne, P.R., Vogel, N., Deino, A.L., Sharp, W.D., Becker, T.A., Jaouni, A.R., Mundil, R., 2005. Alder Creek sanidine (ACs-2): a quaternary 40Ar/39Ar dating standard tied to the Cobb Mountain geomagnetic event. Chem. Geol. 218, 315–338. http://dx.doi.org/10.1016/j.chemgeo.2005.01.005.
Payen, P., Argant, J., Crégut-Bonnoure, E., 1990. Le gisement moustérien de l'abri Moula (Soyons, Ardèche). Ardèche archéologie 7, 3–9.
Prescott, J.R., Hutton, J.T., 1988. Cosmic ray and gamma ray dosimetry for TL and ESR. Int. J. Radiat. Appl. Instrum. Part D. Nucl. Tracks Radiat. Meas. 14, 223–227. http://dx.doi.org/10.1016/1359-0189(88)90069-6.
Richard, M., Falguères, C., Pons-Branchu, E., Bahain, J.-J., Voinchet, P., Lebon, M., Valladas, H., Dolo, J.-M., Puaud, S., Rué, M., Daujeard, C., Moncel, M.-H., Raynal, J.-P., 2015. Contribution of ESR/U-series dating to the chronology of late Middle Palaeolithic sites in the middle Rhône valley, southeastern France. Quat. Geochronol. 30, 529–534. http://dx.doi.org/10.1016/j.quageo.2015.06.002.
Sambridge, M., Grün, R., Eggins, S., 2012. U-series dating of bone in an open system: the diffusion-adsorption-decay model. Quat. Geochronol. 9, 42–53. http://dx.doi.org/10.1016/j.quageo.2012.02.010.
Sanzelle, S., Pilleyre, T., Montret, M., Faïn, J., Miallier, D., Camus, G., de Goër de Hervé, A., Defleur, A., 2000. Datation par thermoluminescence :étude d'une corrélation chronologique possible entre le maar de La Vestide-du-Pal et un niveau de téphra de La Baume-Moula-Guercy (Ardèche, France). C. R. Acad. Sci. - Ser. IIA - Earth Planet. Sci. 330, 541–546. http://dx.doi.org/10.1016/S1251-8050(00)00171-3.
Saos, T., 2003. Cadre stratigraphique, paléoclimatique et géochronologie du Languedoc-Roussillon au cours du Pléistocène supérieur d'après l'étude des remplissages de grottes (PhD Thesis) Université de Perpignan.
Saos, T., Djerrab, A., Defleur, A.R., 2014. Étude stratigraphique, sédimentologique et magnétique des dépôts Pléistocène moyen et supérieur de la Baume Moula-Guercy (Soyons, Ardèche). Quaternaire 25, 237–251.
Shackleton, N.J., 1969. The last interglacial in the marine and terrestrial records. Proc. R. Soc. B Biol. Sci. 174, 135–154. http://dx.doi.org/10.1098/rspb.1969.0085.
Storm, P., Wood, R., Stringer, C., Bartsiokas, A., de Vos, J., Aubert, M., Kinsley, L., Grün, R., 2013. U-series and radiocarbon analyses of human and faunal remains from Wajak, Indonesia. J. Hum. Evol. 64, 356–365. http://dx.doi.org/10.1016/j.jhevol.2012.11.002.
Tillet, T., Bernard-Guelle, S., Delfour, G., Bressy, C., Argant, J., Lemorini, C., Guibert, P., 2004. JIBOUI, station moustérienne d'altitude dans le Vercors (Drôme). l'Anthropologie 108, 331–365. http://dx.doi.org/10.1016/j.anthro.2004.10.002.
Valensi, P., Crégut-Bonnoure, E., Defleur, A., 2012. Archaeozoological data from the Mousterian level from Moula-Guercy (Ardèche, France) bearing cannibalised Neanderthal remains. Quat. Int. 252, 48–55. http://dx.doi.org/10.1016/j.quaint.2011.07.028.